Zeitschrift: Eclogae Geologicae Helvetiae
Herausgeber: Schweizerische Geologische Gesellschaft
Band: 96 (2003)
Heft: 2

Artikel: Shallow structure of the lower Rossboden Glacier and its moraine dam (Valais, Swiss Alps)
Autor: Oberholzer, Peter / Vonder Mühll, Daniel / Ansorge, Jörg
DOI: https://doi.org/10.5169/seals-169022

0012-9402/03/020299-14
DOI 10.1007/s00015-003-1082-5
Birkhäuser Verlag, Basel, 2003

Eclogae geol. Helv. 96 (2003) 299–312

Shallow structure of the lower Rossboden Glacier and its moraine dam (Valais, Swiss Alps)

PETER OBERHOLZER[1]*, DANIEL VONDER MÜHLL[1,2] & JÖRG ANSORGE[3]

Key words: Dead ice, moraine dam, ground ice melting, debris flows, refraction seismics, DC resisitivity, photogrammetry

ABSTRACT

The goal of this study was to assess the present terminus position of Rossboden Glacier (Simplon area, eastern Valaisan Alps, Switzerland) and to detect potentially unstable zones within the frontal moraine dam. On the dam, in the forefield and on the debris-covered tongue, refraction seismic and DC resistivity measurements were carried out in the summer of 1997. The changes of the glacier surface and its elevation between 1980 and 1996 were reconstructed by photogrammetrical means. The active glacier tongue is presently overthrusting a dead ice mass, thus remobilising the dead ice. This makes the definition and localisation of an actual ice margin difficult. In downvalley direction from the dead ice mass, the ground ice content decreases continuously. The distribution of seismic velocity and electric resistivity values reveals zones of loosely bedded or water-saturated till – both features known to be potential starting points of mass movements – mainly in the moderately inclined forefield of the glacier, but not in the steep face of the moraine dam. Both zones are not regarded as unstable at present.

ZUSAMMENFASSUNG

Das Ziel dieser Arbeit war, die aktuelle Lage des Zungenendes des Rossbodengletschers (Simplongebiet, östliche Walliser Alpen) zu bestimmen und potentiell instabile Zonen in seiner Moränenbastion zu ermitteln. Dazu wurden im Sommer 1997 auf dem Damm, im Vorfeld und auf der schuttbedeckten Zunge des Gletschers refraktionsseismische und geoelektrische Messungen durchgeführt. Durch Luftbildauswertung wurde das Bewegungsverhalten des Gletschers und die Veränderung seiner Oberfläche zwischen 1980 und 1996 erfasst. Die aktive Gletscherzunge fährt offenbar auf eine vorgelagerte Toteismasse auf, wodurch diese reaktiviert wird. Damit wird die Definition eines eigentlichen Zungenendes erschwert. Talwärts nimmt der Eisgehalt im Untergrund kontinuierlich ab. Die Verteilung der seismischen Geschwindigkeiten und elektrischen Widerstände zeigt, dass potentiell instabile Zonen (locker gelagertes oder wassergesättigtes Material) hauptsächlich im flachen Teil des Gletschervorfeldes vorhanden sind, nicht aber in der steileren Aussenseite der Moränenbastion. Beide Zonen können heute als stabil bezeichnet werden.

1. Introduction

Over the last decades, debris flows originating from moraine dams and/or glacier forefields have severely damaged villages and traffic lines in the Alps in several cases (Haeberli et al. 1990). Such potentially dangerous moraine dams were usually piled up during Holocene glacier advances, in the middle of the 19th century (Little Ice Age) and around 1925 by glaciers with a high sedimentary input. Particularly high danger results from lakes dammed by moraine material in front of a glacier, at its margin, or in the periglacial area (Haeberli 1992). Well known examples are those at Gruben Glacier with outbursts in 1968 and 1970 (Röthlisberger 1979; Lichtenhahn 1979; Kääb & Haeberli 1996) and at Lake Sirwolte with an outburst in 1993 (Haeberli 1999), both situated in the Valaisan Alps and near Rossboden Glacier. In both cases, the outburst of a moraine-dammed proglacial lake flooded the drainage channels and eroded several 100'000 m^3 of material along its flowpath downvalley.

The dynamics of a glacier with advancing and retreating periods in combination with a thick debris cover causes complex sedimentary structures in the ice and till at the glacier end. Active glacier ice and dead-ice bodies cut off from the active glacier and protected by the till for many years can interact in complicated processes. This makes it very difficult to define an actual terminus of the active glacier ice.

Rossboden Glacier is a 3 km long valley glacier in the eastern Valaisan Alps, Switzerland (Fig. 1). It flows down from 4000 to about 2000 m a.s.l. The steepest part (~35°) is heavily

[1] Laboratory of Hydraulics, Hydrology and Glaciology (VAW), Swiss Federal Institute of Technology (ETH), Gloriastr. 37/39, CH-8092 Zürich, Switzerland
[2] Rektorat, Universität Basel, Petersgraben 35, 4051 Basel, Switzerland
[3] Institute of Geophysics, Swiss Federal Institute of Technology (ETH), ETH-Hönggerberg, CH-8093 Zürich, Switzerland
* corresponding author, present address: Institute of Isotope Geology and Mineral Resources (IGMR), Swiss Federal Institute of Technology (ETH), Sonneggstr. 5, CH-8092 Zürich, Switzerland. E-mail: oberholzer@erdw.ethz.ch

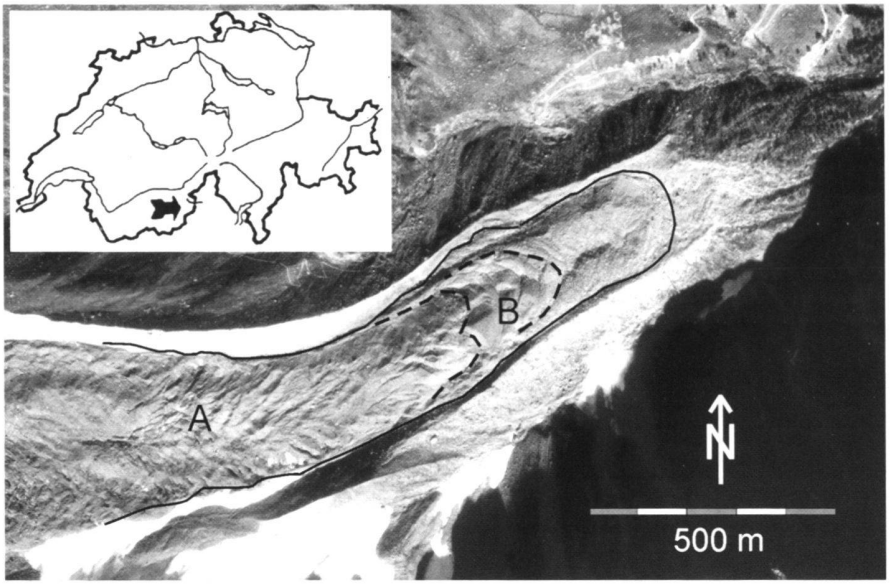

Fig. 1. Aerial photograph of the investigated lower part of Rossboden Glacier from September 1986. Crevasses are visible as linear structures in the upper part (A), and pressure ridges as curved lines downglacier (B). The dashed lines mark the boundaries of these zones in downglacier direction. The tongue-shaped solid line represents the 1925 moraine, as plotted in Figs. 2,7 and 8. Inset: Map of Switzerland with location of Rossboden Glacier. (Photograph taken by V+D (Swiss Directorate for Cadastral Surveying) for VAW/ETH Zürich).

crevassed. The lower part is less inclined, tongue-shaped and almost entirely debris-covered. It is underlain by a thick bed of glacial sediments, as must be assumed from the surrounding morphology. While the high lateral moraines were last reached by the 1850 advance, the frontal moraine dam was covered again in 1925 (Hantke 1983). The large amounts of debris are provided by the strongly fractured rock walls particularly along the orographic right side of the glacier. As part of the lower Penninic Bernhard Nappe, the bedrock in this area consists mainly of gneisses and schists (Bearth 1973). As one of only a few Swiss glaciers, Rossboden Glacier was advancing until recently (Hoelzle et al. 1998), but its presently assumed terminus is situated still far behind the large frontal moraine of 1925 (Figs. 1 and 2A). Because of the debris cover, the exact position of today's terminus is difficult to determine. In recent years, a considerable amount of dead-ice has melted in the forefield (Fig. 2A). As a consequence, the surface immediately behind the old dam subsided and several local depressions formed. Even a small lake was observed in the forefield in summer 1996 (Oberholzer & Salamí 1998). In the text, the term "forefield" refers to the area between the ice visible at the surface at the time of data acquisition and the dam. The term "frontal dam", in turn, includes the slope which limits the former ice extent at the front of the tongue-shaped debris body and towards the high lateral moraines. This surface, with its upper end at an elevetion of approximately 1930 m a.s.l., is steeper than the forefield. It was one of the major goals of this study to define the exact extent of the forefield and of its transition zone to the active ice. Thus, the terms forefield and dam refer to the middle and the lower part of the study area rather than to an exactly defined feature or zone. These parts are indicated in Figure 2A. An earlier study by Müller (1983) investigated the ice distribution in the forefield of today's glacier by means of sledgehammer refraction seismics, radio echo soundings, bottom temperature of snow cover (BTS) measurements as well as kinematic measurements of surface points and aerial photographs. He reported that the active glacier advanced at an average rate of 48.2 m/a between 1968 and 1981, overthrusting and reactivating dead ice deposited during an earlier advance.

In the present study, the structural investigations of the forefield and moraine dam were extended upglacier using "classical" geophysical methods applied in periglacial areas: refraction seismics with both explosives and sledgehammer, and DC resistivity soundings. The number of measurements was strongly increased compared to the study by Müller (1983). The main objectives were:

(1) to assess the stability of the frontal moraine dam (Fig. 2A) by determining the sediment thickness, degree of consolidation and water saturation, and thus to localise potential zones of failure and mass movement;
(2) to localise ice masses in the subsurface of the forefield (Fig. 2A) in order to clarify the relative position and interaction of the active glacier tongue and the dead glacier ice;
(3) to localise the present frontal ice margin of the active glacier;

In addition, BTS measurements, photogrammetrical investigations, radio echo soundings and seismic ambient noise measurements (Fäh et al. 1997) were carried out for complementary information related to the above listed goals (Oberholzer & Salamí 1998). All the data discussed here except the BTS were collected in July and August 1997 when the entire investigated area was free of snow. BTS was measured in March 1997. All information on elevation of the ice masses is given as

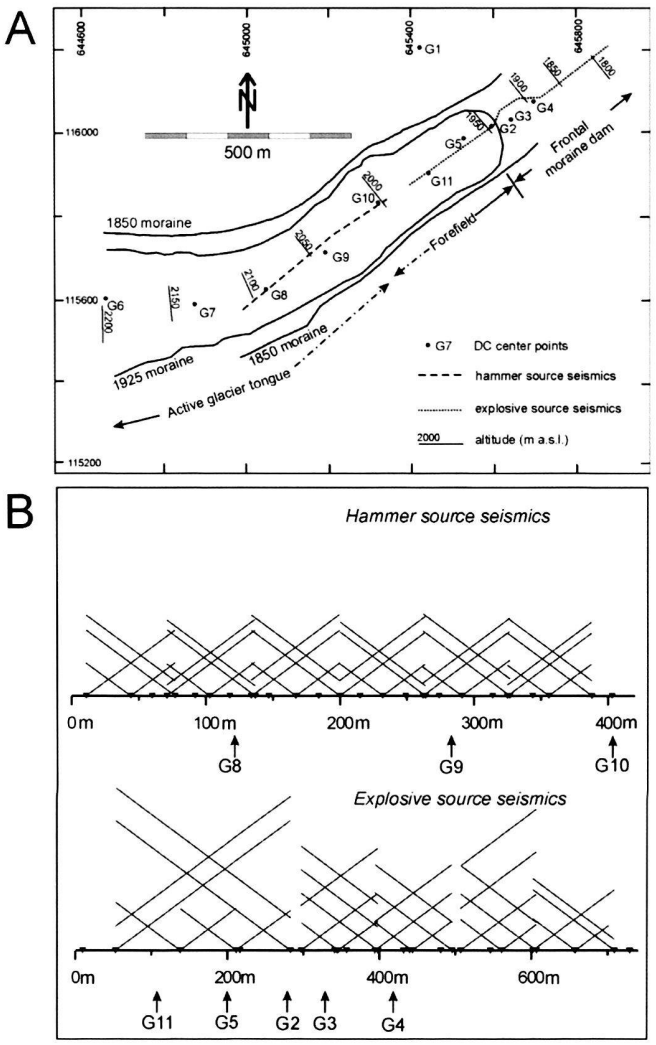

Fig. 2. (A) Overview of the measurement locations with seismic lines and centre points G of DC soundings. Altitude indications refer to the respective point on the seismic line, they are no contour lines. For clarity of the figure, seismic ambient noise points are not shown. They are situated along the seismic line between 1940 and 2140 m.a.s.l. Coordinates refer to the Swiss national coordinate system.
(B) Schematic overview of the shot and recording coverage. Thin black lines indicate the geophone spread for every shot or hammer blow. The horizontal axis is the profile distance of the seismic lines, increasing downhill in each section (note different distance scales). Black triangles on the axis represent shot or blow points. For orientation, the positions of the DC centre points G (partially projected onto the seimic line, see Fig. 2A) are given.

altitude above sea level as measured during the field campaign by terrestrial survey, which is, due to the geomorphic dynamics, not necessarily the same altitude as in the older official Swiss topographic map.

Similar investigations were performed on the moraines of Gruben Glacier (Vonder Mühll et al. 1996) and Dolent Glacier (Lugon et al. 2000).

Tab. 1. Typical ranges of P-wave velocity and specific electric resistance (modified after Haeberli et al. (1990), derived from studies in high-altitude Quaternary deposits).

Material	*Seismic velocity v_p (m/s)*	*Specific resistance ρ_s (kΩ m)*
dry, coarse debris	300-900	1 - 10
till, +/- consolidated or wet	800-2000	1 - 10
Avalanche debris, firn patches	2000-3000	10^3 - 10^4
ice-rich till, permafrost	2000-4500	10 - 10^3
glacier ice	3300-3800	10^4 - >10^5
groundwater in debris/till	1500-2500	0.5 - 2
bedrock, depending on degree of cleavage	2500-4000	strongly varying
solid bedrock	4000-6000	strongly varying

2. Methods

2.1 Refraction seismics and seismic noise analysis

Seismic methods are well suited for studies on ice-containing debris because of the clear velocity differences of the involved materials. Typical compressional (P-) wave velocities for different glacier-related materials are given in table 1.

The near-surface cover at the Rossboden site (glacier, forefield and frontal moraine) consists of coarse debris which causes a high level of incoherent signal-generated noise after an explosive detonation or a hammer blow. Therefore, reflection seismics is not appropriate in such kind of terrain (Musil et al. 2002). Reflections and diffractions from different layers and inhomogenities at various depths and directions are recorded at the same time. In refraction seismics, only first arrivals of waves are picked, which are not affected by signal-generated noise but are only attenuated.

The seismic investigations had two objectives. First, to detect any layering within the moraine. Second, to assess the distribution of ice in the subsurface of the forefield. To meet these objectives, explosives and a sledgehammer were used as sources of energy. The explosive source, in combination with a wide geophone spacing (5 and 10 m) and a large observation distance at a limited number of recording channels, provides a deeper penetration, but also a lower resolution of layering and velocity than hammer blows at shorter distance intervals. It was, therefore, applied in the area of the frontal dam and the forefield (Fig. 2A) where a thick sediment body was expected,

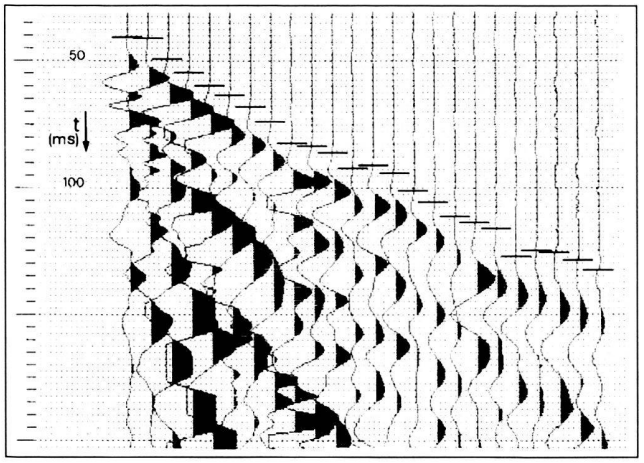

Fig. 3. Example of a seismogram section (shot 5 in Fig. 4A). Horizontal marks are the first arrival picks as used for the time-distance plots. This record section led to the following velocities: v_1= 700 m/s (shotpoint to geophone 5); v_2= 1300 m/s (geophones 5 to 24). Note that this figure shows travel time versus geophone number, not versus distance. The equal geophone distances in the figure are given by the plotting instrument. Uphill direction is on the right-hand side.

Tab. 2. Shear velocities calculated from ambient seismic noise analysis at several elevations. Note that these values are average values for the entire sediment bed and based on the crude assumption of a uniform sediment thickness of 100 m. Therefore, only a relative comparison to P-velocities should be made.

Elevation (m a.s.l.)	*S-wave velocity V_S (m/s)*
1940-1990	600-650
1955	300
2010-2055	250-500
2005, 2090-2140	650-700

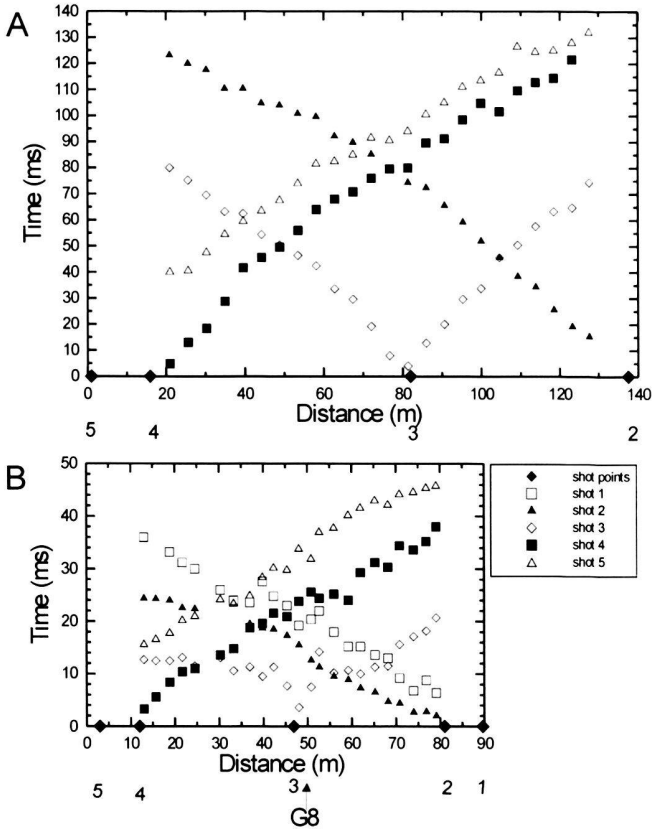

Fig. 4. Examples of a time-distance plot for (A) an explosive source profile (recorded between 1775 and 1810 m a.s.l., see Fig. 2A; shot 1 was not recorded), and (B) a hammer source profile (recorded between 2090 and 2100 m a.s.l., near G8, see Fig. 2A). (Note that time and distance scales are different in A and B. However, the time/distance ratio is the same in both plots so the slopes of the branches, i.e. the apparent velocities, can be compared) The legend is valid for both graphs. Uphill direction is on the righthand side in both panels.

in order to gain information on the stability of the moraine. The sledgehammer on the other hand (geophone spacing 3 and 5 m) provided a better resolution but a shallower penetration. Hence, this source was used for the localisation of small-scale, near-surface material changes in the glacier forefield. Seismic signals were recorded with a 24-channel ABEM Terralog instrument. Shot sizes ranged between 0.1 and 0.8 kg per shot. For both types of seismic measurements, shot points were chosen at each end of every geophone spread, at its centre point, and in most cases in the prolongation of the spread at an appropriate distance. A sketch of the coverage of the shots is given in figure 2B. The largest observation distances with explosives and hammer were 290 and 83 m, respectively. First arrival times were picked directly in the field to check the quality of the data and later re-picked for the final dataset. These first-arrivals were plotted in time-distance diagrams. Apparent seismic velocities were determined by visually fitting lines through the data points. The refractor depths were determined using the cross-over method, intercept method (e.g. Dobrin & Savit 1988), and, where reversed shots were available, the plus-minus method (Hagedoorn 1959). Topographic corrections for the cross-over and intercept methods were not applied because they would have been significantly smaller than the observed scattering of the first arrival times. Due to the limited amount of data and difficult data transfer from the recording instrument to a computer all data were processed directly on the ABEM Terralog. Examples of a seismogram section and time-distance plots are shown in fig-

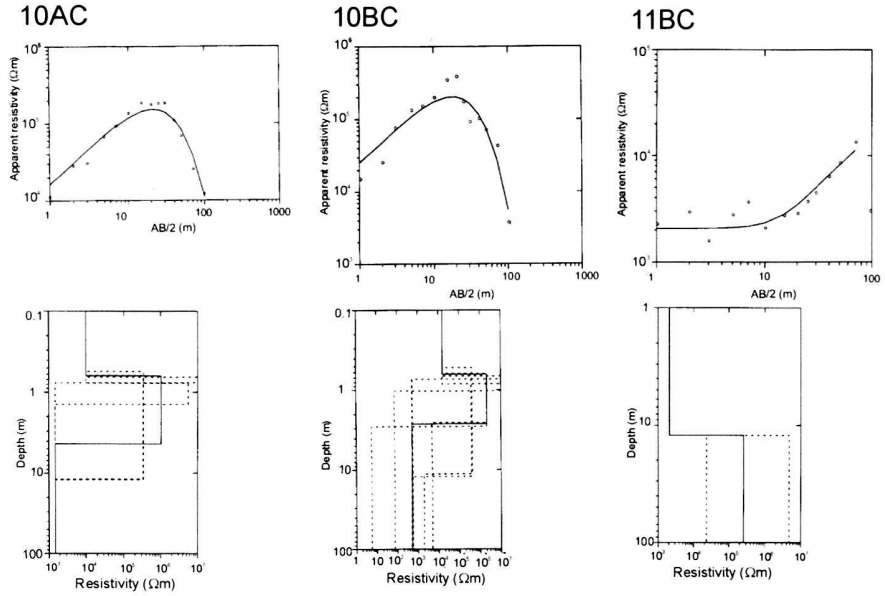

Layer	Depth (m)	ρ s (kΩ m)	Characteristics
1	<1	10	coarse debris
2	<12	310-47'000	ice
3		1.5	water-rich till

Layer	Depth (m)	ρ s (kΩ m)	Characteristics
1	<1	16	coarse debris
2	<11	370-120'000	ice
3		<4	till

Layer	Depth (m)	ρ s (kΩ m)	Characteristics
1	12	2	till
2		23-4700	ground ice

Fig. 5. Examples of DC data (for locations of G10 and G11 see Fig. 2A). Upper panels: Open circles are measured data points, the black line is the calculated fitting curve. Middle panels: The calculated equivalent layer models. The mean resistivity model (solid line) was chosen for further interpretation and Tab. 3. The tables give the depth and resistivity ranges of the computed possible layer models. 10AC and BC are the Hummel branches at sounding point G10.

ures 3 and 4, respectively. The refractor points resulting from each interpretation method were plotted in a topographic section along the seismic line at their respective depth below surface and with velocity contrast. These points were then combined to a layer model supported by all three methods by interpolation between points and correlation of horizons with similar P-wave velocity contrast.

Measurements of the ambient seismic noise and analysis of the polarisation of the noise wavefield is another valuable technique to determine the gross structure and shear (S)-wave velocity of shallow sediments (Fäh et al. 1997; Nakamura 1989). The polarisation is determined in terms of the ratio of the frequency spectra between horizontal and vertical shear-wave components over a given frequency range and averaged over several time intervals. The dominant frequency given by the highest ratio is directly related to the average shear-wave velocity and the thickness of unconsolidated sediments above an interface with clear velocity contrast. However, these two values cannot be determined independently. Results are shown in table 2.

2.2 DC resistivity sounding

The aim of the DC (direct current) resistivity soundings was to determine the variation of the specific electric resistance ρ_s with depth. ρ_s varies strongly between dry and wet loose material and between ice and unfrozen material and, therefore, is a highly appropriate parameter to detect ice and water-saturated zones in the subsurface. DC resistivity sounding allows to separate and detect layers of different DC resistivities (Ωm), especially low-resistivity layers in glacial environments. Water is an electrical conductor, due to the presence of freely moving ions, in contrast to ice, which acts as an insulator because ions cannot move. The measured sounding curve of electrode spacing versus apparent resistivity was fitted iteratively to several one-dimensional resistivity models, using the software Resix Plus (Interpex Ltd., 1997); for basics of the method see e.g. Koefoed (1979). The average values of the modeled layer resistivities were chosen for the structural interpretation. Figure 5 shows examples of DC sounding curves and resistivity models. The result of this inversion of data is a layered model for the subsurface at the centre of the electrical sounding. Typical resistivity values for glacial and periglacial environments are given in table 1. The method has often been applied to permafrost (e.g. King 1984; Vonder Mühll 1993), as well as to glaciers (e.g. Haeberli & Fisch 1984).

A total of 10 soundings (centre points G in Fig. 2A) were carried out with electrode spacings from 200 to 400 m between 1890 m a.s.l at the front of the moraine and 2200 m a.s.l. on the debris-covered part of Rossboden Glacier (Fig. 2A). In addition, one calibration sounding was carried out on bedrock with a soil cover of ca. 2 m outside the glacier (sounding G1, see Fig. 2A and Tab. 3). The profiles were set up approximately perpendicular to the former flow direction of the glacier, i.e. perpendicular to the seismic line. To determine lateral differences, a combination of Schlumberger and Hummel (asymmetrical Schlumberger) array was used (Milsom 1996). At four soundings (Fig. 2A: G5, G8, G10, G11) marked differences of the two Hummel-branches were observed and processed accordingly.

DC resistivity sounding				Refraction seismics		
Sounding No.	Layer thickness (m)	ρ_s (kΩm)	Material	Layer thickness (m)	v_p (m/s)	Material
G1	1	1	soil			
	10	5.2	solid bedrock			
	∞	1.6	fractured/water-rich bedrock			
G2	3	2.8	loose till			
	7	35	ice/till	8 to 10	<800	loose till
	∞	0.5	water-rich till	∞	2200	water-rich till
G3	1	3	soil			
	1	0.6	water-rich till			
	6	4.4	loose till	5 to 8	<800	loose till
	∞	2.1	fairly consolidated till	∞	1000	fairly consolidated till
G4	1	2.9	loose till, wet			
	5	5	loose till	6	<800	loose till
	∞	3.4	fairly consolidated till, wet	∞	1000	fairly consolidated till
G5	2	6.2	blocky debris			
	6	3.9	loose till	8 to 10	<800	loose till
	4	62	ice/till	∞	2400	ice/till
	∞	0.9	water-rich till			
G6	1	120	ice	-		
	10	3500	ice			
	13.5	100	ice			
	∞	19	water-rich till			
G7	2	340	ice	-		
	8.5	1700	ice			
	14	640	ice			
	∞	13	wet till			
G8				<5	<800	loose till
	20	80	ice/till	15	2600	ice/till
	∞	1.5	water-rich till	∞	3600	ice
G9	0.5	2.4	loose till	<5	<800	loose till
	10	150	ice	4	2000	consolidated or water-rich till
	∞	0.5	water-rich till			
G10	0.5	10	loose till, wet	5	<800	loosely bedded till
	4	1000	ice			
	∞	1.4	water-rich till			
G11	1	7.2	blocky debris			
	1	1.1	loose till			
	6	57	ice/till	6 to 8	<800	loose till
	∞	0.9	water-rich till	∞	2400	ice/till

Tab. 3. Comparison of layer properties derived from the selected DC resistivity-layer model (solid line in Fig. 5) and refraction seismics at the intersection of profiles. At the positions of the soundings G6 and G7 no seismic survey was done. G1 is a reference profile for the calibration of the DC soundings, measured outside the investigated area. Material interpretation is based on Tab. 1.

2.3 Bottom temperature of snow cover (BTS)

The objective of the BTS survey was to gain information about the lateral extent of permafrost or ground ice in the forefield of Rossboden Glacier and its moraine dam. The measurements were carried out in the winter preceding the other geophysical field work so the BTS results could be used to optimise the position of the geophysical arrays. The BTS is influenced by the long-time thermal regime of the shallow underground. A snow cover of at least 0.8 m prevents the BTS from following high frequency temperature variations of the atmosphere (air temperature and radiation, Haeberli 1973; Haeberli & Patzelt 1982; Hoelzle et al. 1999). BTS values are classfied empirically as follows (Haeberli 1973): BTS > -2°C: ground ice or permafrost not probable; -2°C > BTS > -3°C: ground ice or permafrost possible; BTS < -3°C: ground ice or permafrost probable. A total of 128 points were measured along four parallel lines from 1850 to 2250 m a.s.l. Because of avalanche danger, the area outside of the lateral moraines could not be investigated.

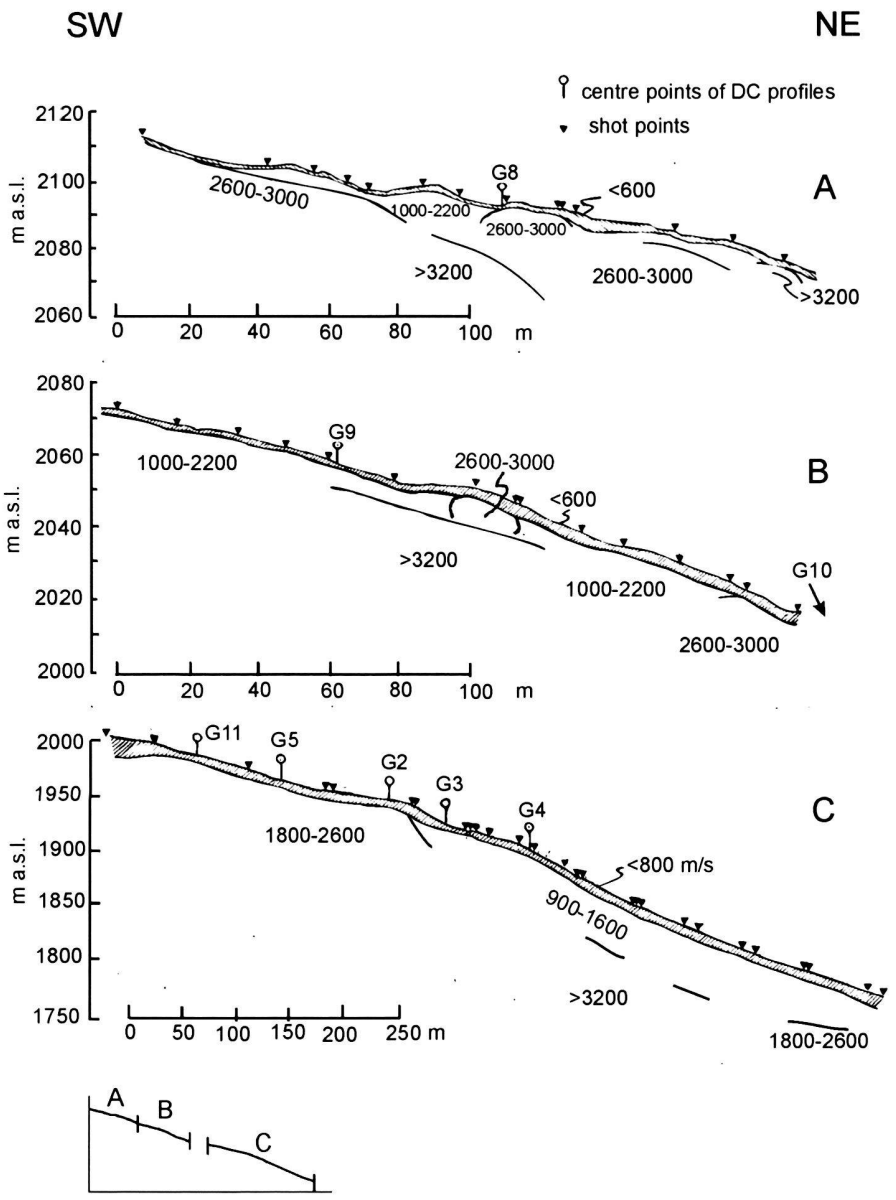

Fig. 6. Results of refraction seismics. Layer boundaries are supported by all three interpretation methods mentioned in the text. (A) and (B): hammer seismics, (C): explosive source seismics. Note that vertical and horizontal scales in (C) are different from those in (A) and (B). The relative positions and dimensions of (A), (B) and (C) are shown in the lower left corner. The hatched area is the surface layer. (numbers are P-wave velocities in m/s)

2.4 Photogrammetry

A photogrammetrical survey was carried out in order to quantify surface motion and variations of the ice margin position during the 14 years since the last study in this area by Müller (1983). For this purpose, aerial photographs taken between 1983 and 1996 were analysed.

Photogrammetry uses pairs of aerial photographs taken at the same time from slightly different positions. The overlapping area of the pictures is analysed stereoscopically for three-dimensional information on the surface and can be analysed, e.g., using simultaneous monoplotting in a multitemporal stereo model. For details on this method in glacial surveys see Kääb (1996). Four different parameters were recorded or calculated, respectively: (a) absolute position of surface features, (b) topographic sections of the surface, (c) horizontal displacements, and (d) vertical displacements.

3. Results and interpretation

3.1 Refraction seismics and seismic noise analysis

The seismic data show refracted signals of varying quality depending on source efficiency and attenuation. Some travel time branches appear on one shot record but not on the corre-

sponding reversed one and, therefore, are uncertain. The lower boundary of the surface layer can be identified everywhere by both the explosive and sledgehammer data. A second or even third interface can be found in a number of shots, but not always on the reversed shot records, where they are expected. The fact that refractors appear discontinuously indicates strong and numerous small-scale inhomogeneties.

A) Explosive source seismics

Figure 6C shows the continuous surface layer of loose moraine debris (<800 m/s) with an average thickness of 9 m in the forefield and on the frontal moraine dam. The velocities of a second layer are very variable and increase towards the glacier (900-1600 m/s to 1800-2600 m/s). There is a possible third layer at a depth of about 50 m with average apparent velocities higher than 3200 m/s. This deep, high-velocity refractor possibly representing bedrock was found in two shots upglacier and downglacier, but never on a truly reversed profile, therefore the true velocity cannot be determined. In the upper part of the seismic line (i.e. in the forefield), the moraine is obviously too thick to detect the bedrock with the used size of explosive sources. Its minimum thickness can be estimated from the surrounding surface slope of the bedrock to be around 100 to 150 m.

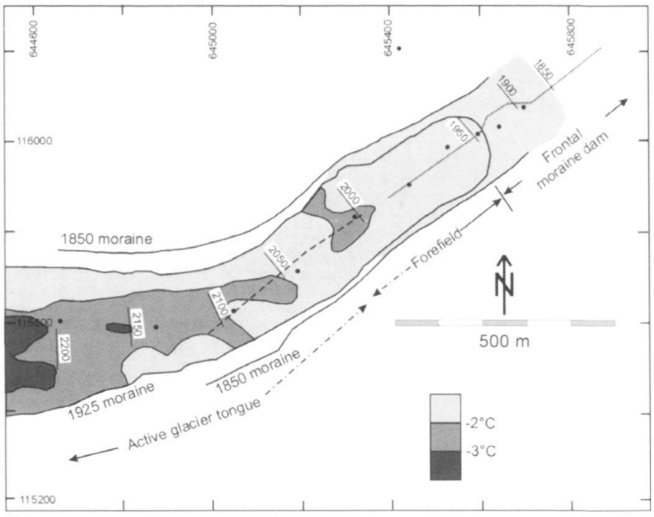

Fig. 7. Distribution of the bottom temperature of snow cover (BTS) in early March 1997, derived from 128 measuring points. DC centre points (black dots) are given for orientation. Temperature intervals are shown according to their significance regarding ground ice occurrence: BTS>-2°C, ground ice or permafrost not probable; BTS<-2°C, ground ice or permafrost possible; BTS<-3°C, ground ice or permafrost probable.

B) Sledgehammer source seismics

The picture resulting from the sledgehammer source seismics (Fig. 6A, B) is considerably less homogeneous than that based on the explosive source. This is mainly due to the changing character of the underground as the seismic line proceeds from the forefield towards the glacier. Another reason, though, might be the larger scatter of travel time picks on the seismic signals with a lower signal-to-noise ratio generated by the sledgehammer. The loose moraine material at the surface (<600 m/s) with an average thickness of 2 m is continuous. Its seismic velocity is clearly lower than that obtained further downglacier. The second layer is characterised predominantly by velocities between 1000 and 2200 m/s (Fig. 6). Lateral variations of velocity derived from clearly separated traveltime branches of 2600 m/s and higher (Fig. 6A and B) are attributed to bodies with higher velocity embedded in the low-velocity material. Their length varies from 15 to 80 m, but their thickness is unknown. Beneath G8 (Fig. 6A), an extended layer with velocities higher than 3200 m/s is detected beneath the top two layers which is attributed to the active glacier tongue. Although the moraine bed is expected to be thinner beneath the forefield than near the dam, the hammer source provided not enough energy to reach bedrock.

C) Ambient Seismic noise analysis

The ambient seismic noise was measured and analysed at twelve points along the centre line of the glacier (Fig. 2A). As mentioned earlier, layer thickness and S-wave velocity (v_S) cannot be determined separately. Since the active seismic data did not provide reliable independent values for the total thickness of subglacial debris and ice above bedrock an average value of 100 m was estimated from the slope of the surrounding bedrock to determine the order of magnitude of average v_S and its variation along the glacier. This provides additional hints on the consolidation of the overall moraine-ice cover above bedrock. Because of the simplifying assumption of subglacial debris thickness the S-wave velocities given in table 2 are not real and can only be used to judge relative structural variations.

3.2 DC resistivity soundings

At the lowermost five soundings G2 to G5 and G11, resistivities are low (<7.2 kΩm) for the uppermost at least 2 m (see Fig. 2A and Tab. 3). They are low or intermediate (<62 kΩm) also in all deeper layers. The five profiles upglacier from G10, however, show no low-resistivity surface layer or only a very thin one. Instead, in the uppermost two layers high values of up to 3500 kΩm were measured. No systematic pattern can be identified in the resistivities beneath the second layer. Thus, the resistivities generally are considerably higher and layers are thicker upglacier from sounding G10.

3.3 Synthesis of seismic and DC resistivity soundings

When comparing the results of the two methods, one has to be aware of the relative orientation of profiles. The electrode

spread of up to 400 m was perpendicular to the seismic line. The DC soundings are interpreted one-dimensionally at their centre points near the seismic line, and the measured data are influenced by subsurface material beneath the entire profile in all directions. For example, an isolated block of ice located significantly off the seismic profile but on the DC profile causes an increase of the apparent resistivity, but is not recognised on the seismic profile. Hence, comparison of seismic and DC resistivity data is difficult where material changes must be expected within short distance.

Average values of both seismic velocities and resistivities for different media are given in table 1. The lower boundary of the surface layer derived from the seismic data in most profiles coincides with a layer boundary in the DC investigations (Tab. 3), but in the latter, more layers have been resolved within the uppermost metres. An important feature of the second layer of the seismic structure is that seismic and DC results differ in the zone where the transition from active glacier ice to ice-free debris must be expected (sounding points G2, G5, G9 and G10, see Tab. 3). There, the resistivities indicate more often the presence of ice (>150 kΩm) or ice-debris mixture (50 to 80 kΩm) than the seismic velocities do. These contradictions could be due to ice occurrences off the seismic line, indicating strong and numerous, short-distance lateral material variations in the subsurface. However, the combination of high resistivity and low velocity may also be indicative of air voids in the subsurface (Hauck 2001) or near-temperate ice conditions with high unfrozen water content.

By comparing DC resistivities and seismic velocities, dry debris cannot be unambiguously distinguished in all cases from unconsolidated debris, neither can wet debris be distinguished from consolidated debris. Intermediate velocities of 1000 to 2600 m/s can be interpreted either as water-rich, ice-rich or consolidated debrist. The corresponding resistivities are either low (<1 kΩm), typical for water-rich till, or high (>35 kΩm), indicating ice-rich till, but not intermediate as in consolidated debris. Thus, the main part of the glacial debris seems to be of a uniform low or intermediate degree of consolidation, but of a varying water and ice content.

3.4 BTS measurements

According to the BTS results of 128 measurements (Fig. 7), the subsurface in the forefield of Rossboden Glacier below 2000 m a.s.l. and in the uppermost part of the frontal moraine is free of ice (i.e., BTS>-2°C). A tongue-shaped zone of intermediate temperature values (compare definition in 2.3) reaches down to 2050 m a.s.l. between the lateral moraines, and an isolated patch of less than -2°C occurs at around 2000 m a.s.l. A laterally continuous zone of cold values ends at 2200 m a.s.l. (Fig. 7) which is considerably higher than the research area for the other geophysical methods. This zone most probably represents active glacier ice, but not necessarily its lowermost occurrence. Müller (1983) detected subsurface ice by BTS measurements within the entire area covered in this study with temperatures consistently lower than -3°C. These data, though, were taken in the winters of 1980/1981 and 1981/1982, the former of which was very cold and both of which did not bring a thick snow cover before January and December, respectively. Thus, the underground had time to cool in late autumn and early winter (Vonder Mühll et al. 1998). This may explain the temperature difference partially, ground ice melting since the early 1980s being a second important contribution.

3.5 Photogrammetry

A distinct change of surface features with time is visible on a series of annual aerial photographs since 1980. In the early and mid 80s a tongue-shaped zone with crevasses and bare ice can be clearly separated from an area further downglacier with arch-like compressive ridges, similar to those typical for rock glaciers (A and B in Fig. 1 of 1986). These features have gradually disappeared by 1997. Now, instead of crevasses and ridges, there are depressions, trenches and river-like structures that dominate the surface in the entire area between the lateral moraines from 1900 to 2200 m a.s.l. A quantitative evaluation of the photographs (for the method see Kääb 1996) confirms these visually observed changes since the early 80s as described in the following paragraphs.

A) Position of surface features

The position and deformation of crevasses and ridges can be traced through time. These zones advanced from 1980 to 1992, the distance between them decreasing from 260 to 120 m. In 1997, the crevassed zone ended at 2010 m a.s.l, about 300 m from the moraine dam. The lower margin of the ridge zone expanded down to 1980 m a.s.l., about 150 m from the moraine dam (Fig. 8A).

B) Horizontal displacements

The significant horizontal displacements of surface elements between 1996 and 1997 as well display two zones with different patterns (Fig. 8B). The upper part to about 2020 m a.s.l. is characterised by downward motion. A second, much smaller part between 2020 and 1980 m a.s.l. shows convergent movements of lower velocities, directed towards the central zone. Between these two zones, velocities are close to zero. The apparent upglacier movements can be interpreted as blocks rolling or sliding down into a depression as a consequence of strong downmelting in the centre and erosion from the steep lateral moraines.

C) Vertical displacements

The zone dicussed in paragraph B between 1980 and 2020 m a.s.l. is characterised by strong subsidence between 1996 and 1997 (Fig. 8C). The pattern of surface elevation changes is sim-

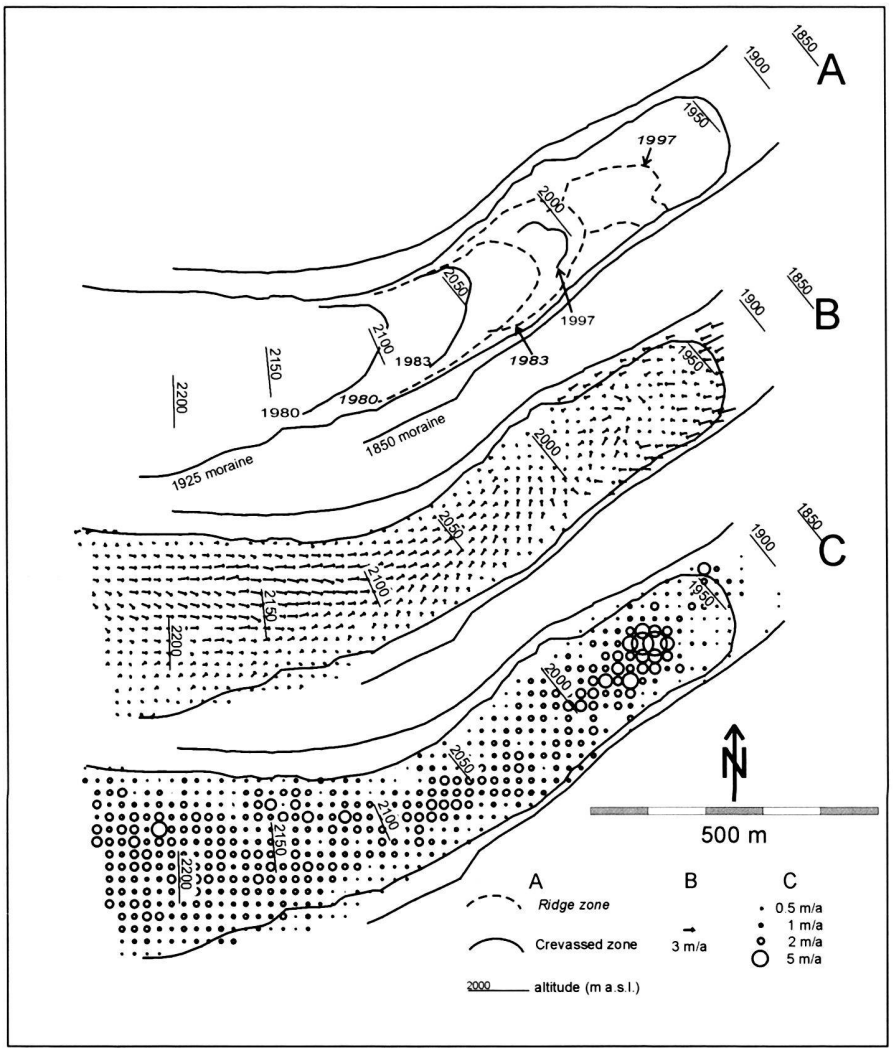

Fig. 8. Results of photogrammetry. (A): Positions of crevassed zone (solid lines) and ridge zone (dashed lines) from 1980 to 1997. The lines represent the downglacier limit of the zones labelled A and B in Fig. 1 (note that Fig. 1 shows the situation in 1986). (B): Vectors of horizontal surface movements between 1996 and 1997. (C): Vertical surface movements from 1996 to 1997. All circles represent subsidence. (For reasons of readability, the points of uplift were omitted. They are very few, however, mainly on the right side of the dam, with amounts less than 1 m.)

ilar to that of horizontal surface movements (Fig. 8B): Two zones of high values are separated by a narrow zone of low values, with the transition at about 2020 m a.s.l. These zones occur at the same positions with respect to the direction of glacier flow. In the upper part, though, high horizontal displacement rates extend further to the orographically left moraine than the vertical displacements. It is unclear what causes this difference. The important feature remains, however, that both vertical and horizontal displacements indicate subsurface dynamics in the same two separate areas.

D) Longitudinal elevation profile

In the topographic sections along the central line of the glacier again two different regions can be distinguished (Fig. 9): A large upper part has continuously subsided since 1980, a smaller lower part was uplifted until 1992, and afterwards subsided too. In 1997, the transition between these zones was at 2010 m a.s.l., corresponding to the lower margin of the crevasse zone in Figure 8A.

These observations unambiguously suggest two large bodies of ice that are at least temporarily decoupled. The upper one, down to approximately 2020 m a.s.l. is likely to be the active glacier tongue, because of its size and shape, subsiding surface, movement pattern and velocities. The lower ice mass, characterised by slow, convergent surface movements, might consist of several dead-ice blocks, in contrast to what would be expected from BTS results. These findings suggest an active glacier that thrusted against the adjacent dead-ice, causing the latter to rise, while the active ice itself was already melting and sinking (around 1992, see Fig. 9). The elevated dead-ice was then exposed to increased melting and its surface began to subside as well (between 1992 and 1997). The interpretation of the observed subsidence between 1980 and 2020 m a.s.l. as ground ice melting is based on the assumption that the average surface layer thickness of 9 m as determined by

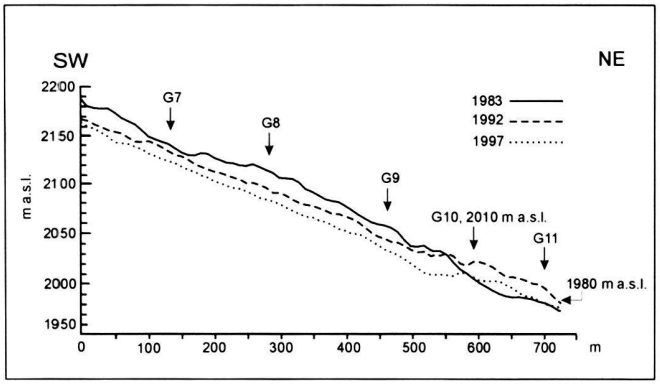

Fig. 9. Results of photogrammetry, longitudinal section of the glacier surface. For better readability, only three years are plotted. The positions of the DC sounding centre points (G) are given for orientation, projected onto the section (see Fig. 2).

seismics does not prevent the process of subsurface ice melting. This assumption is supported by field observations. The mentioned area is characterised by a strong small-scale relief. In the summer of 1997, in several places till had slid down steep slopes of up to 5 m height and bare ice patches of considerable size were visible.

The idea of a dead-ice mass being reactivated by advancing glacier ice was first proposed by Müller (1983). By terrestrial surveying and calculations from air photographs, he found the active ice margin in 1981 at 2140 m a.s.l. and the dead-ice front at 1940 m a.s.l., both advancing until that time (Müller 1983, Fig. 6 therein). Thus, while the active ice margin has advanced since 1981 from 2140 to 2020 m a.s.l., the lower end of the dead ice zone has retreated from 1940 to 1980 m a.s.l. The glacier advance is consistent with the measurements of the Swiss glacier survey (Hoelzle et al. 1998). A moderate retreat of the dead ice mass due to melting seems plausible, even if the dead ice should be pushed further downwards by the advancing glacier.

4.Discussion

4.1 Structure of the moraine bed

The main purpose of this study was to determine the internal structure of the moraine bed in terms of thickness, ice and water content. Results of the seismic and DC soundings indicate a gradual uphill transition from ice-free debris to continuous glacier ice. This is due to the decaying dead-ice in-between the active glacier tongue and the frontal moraine dam. Because the active glacier pushes against the dead-ice, the margin is not clearly determinable by geophysical means. The difference in ice content is not strong in these areas, and neither is the contrast in seismic velocities or DC resistivity. Nevertheless, an estimate of the position of the active to dead ice boundary can be made based on the geophysical evidence. In the seismic profile a continuous body of ice (>3200 m/s; Fig. 6A) is detected at depths of about 20 m beneath G8 at 2094 m a.s.l. This is an upper limit for the altitude of the boundary, though, since the downglacier end of this ice body is unknown. The lowermost occurrence of ice-rich material according to the seismic interpretation is at about 2020 m a.s.l. (Fig. 6B), which is consistent with the photogrammetric evidence.

The DC profiles G8 and G9, which are at 2094 and 2014 m a.s.l, respectively, indicate a thick ice-rich layer (resistivities: 80 and 150 kΩm) at depths of 20 and 10 m, respectively, confirming the seismic estimate of ice occurrence. Other DC profiles at lower positions show ice as well, but dead and active ice can not be clearly distinguished by their resistivity. The lowermost ice deposit identified from the DC soundings is at 1960 m a.s.l. (G5). Further information about the separation of dead and active ice can be obtained from photogrammetric data since there is a difference in movement pattern. The photogrammetric evaluations (Figs. 8 and 9) locate the margin of the active glacier ice with good agreement at 2010 to 2020 m a.s.l. which is about 70 to 80 m lower than the maximum altitude of the ice margin based on seismic data and within the range given by the DC soundings. The photogrammetric dead-ice margin is at about 1980 m a.s.l. and, hence, is again in good agreement with the DC data.

The relatively wide range of shear wave velocity (v_s) values (Tab. 2) reflects the heterogeneous character of the subsurface. The spatial variation of the v_s values is largely congruent with that of the compressional wave velocity (v_p) values as determined from refraction seismics. The rather low v_s values are a consequence of the crude assumption of a constant sediment thickness (h) of 100 m with h being inversely proportional to v_s (Bard & Bouchon, 1985). It can be assumed that h decreases upglacier. The higher up a measurement was taken, the more h is overestimated by our assumption, and the more v_s is underestimated. Nevertheless, the low v_s values presented here are not totally unrealistic. Blankenship et al. (1987) observed shear wave velocities as low as 160 m/s in a subglacial sediment layer underneath ice stream B in Antarctica. Thus, the ambient noise measurements in terms of the variation of high and low values qualitatively confirm the results of both refraction seismics and DC resistivity soundings, although the v_s values are difficult to assign to particular sediment characteristics and should not be regarded as absolute values.

4.2 Hazard potential

In 1987, several hundred debris flows occurred in the Swiss Alps causing large damages. The analysis of the events showed that about 50% of the debris flows were triggered in glacier forefields that some decades ago were still covered by a glacier (Zimmermann 1990). One third started at the lower limit of permafrost. Such events usually are caused by unstable parts of the moraine or loose debris. For the localisation of potentially unstable zones within a moraine, knowing the occurrence of

Tab. 4. Values of the index I for the specification of Quaternary material fitting in one of the two categories listed in paragraph 4.2. I is based on electrical resistivity ρ_s and p-wave velocity v_p (see text for details).

Location, depth	ρ_s *(kΩm)*	v_p *(m/s)*	*Index I*
G2, > 10 m	0.5	2200	0.2
G5, > 12 m	0.9	2400	0.4
G2, <10 m	35	600	120
G3, < 8 m	4.4	600	15
G4, < 6 m	5	400	25
G10, < 5 m	1000	400	498
G11, < 8 m	57	700	162

water-saturated and very loose or highly porous material is of major interest. Their existence and location are the most important parameters for the triggering of mass movement in moraine material (Haeberli 1992; Vonder Mühll et al. 1996; Lugon et al. 2000; Huggel 1998).

Water-saturated Quaternary sediments are characterised by intermediate seismic velocities of 1000 to 2000 m/s and resistivities in the order of 1 to 10 kΩm, depending on the resistivity of the water (Tab. 1). Dry and loosely bedded debris with high porosity or cavities has lower velocities of <900 m/s and unusually high resistivities above 10 kΩm (Vonder Mühll et al. 1996; Hauck 2001). Within water-saturated zones in Quaternary material (e.g. glacial till) one can expect nominal values for P-wave velocity [m/s] of a similar order of magnitude as for the DC resistivity [Ωm], i.e. approximately 2000 m/s and 2000 Ωm, respectively. Zones with low P-wave velocities in general indicate loose material. In combination with a high DC resistivity of more than 10 kΩm, such areas represent bodies with a lot of air voids between boulders. In such material, the nominal value for the DC resistivity [Ωm] is much larger than for the P-wave velocity [m/s].

In order to gain a relationship between seismic and DC resistivity data with regard to water saturation and porosity, Vonder Mühll et al. (1996) deduced an empirical index I defined as

$$I = \mathrm{r} \cdot \frac{\rho s[\Omega m]}{v_p[m/s]}$$

where r equals 1 if ρ_s is decreasing with depth, and 2 if it is increasing. The derived value of I for loose sediments allows to assign the underground to one of two categories:

(a) zones with $v_p > 1300$ m/s and $I < 2$ are highly water-saturated.
(b) zones with $v_p < 900$ m/s and $I > 10$ are of high porosity or containing voids without groundwater filling.

Thus, I indicates if the investigated material is either water-saturated or contains large air voids. Note that ice-rich till should not fit in either category since it is neither very porous nor water-rich. Calculating I for the data of this study, seven zones fitting into one of the two categories can be identified along the profile (Tab. 4). Their depth distribution is as one expects: Wet zones (at G2 and G5, Fig. 2A) are situated at depths greater than 10 m, the porous zones (at G2, G3, G4, G10 and G11) are part of the surface layer above 10 m depth.

Besides the degree of water saturation and of porosity, the surface slope and the thickness of the potentially unstable zones are important factors, too, for hazard potential. On Rossboden Glacier, dry porous material (I>10) was localised mainly in the surface layer, the thickness of which is highest in the steep frontal part of the moraine dam (Figs. 2A, 6) with an average of 9 m. Underneath, the till is of intermediate consolidation. Water-saturated zones (I<2) were found in the less steep forefield containing dead-ice remainings. Their thickness cannot be inferred from the geophysical results. Hence, because wet and loose material exists in steep terrain, the front of the moraine dam could be regarded as a possible origin of debris flows. With an average slope of 30%, its surface is less steep, though, than at other sites where lake outbursts have occurred, such as at Gruben Glacier (e.g. Röthlisberger 1979). While in the steepest part of the Rossboden Glacier frontal moraine the slope is roughly 40 % (between 1800 and 1900 m a.s.l.), it is 70 % at Gruben Glacier, according to the Swiss topographic map. Furthermore the surface on the moraine dam at Rossboden shows no signs of large recent mass movements such as deep channels or levees and is covered with grass, bushes and trees which testifies to a stable surface over the last decades. Thus, the moraine dam at Rossboden Glacier can, under the present conditions, be regarded as relatively safe with respect to mass movement. If, however, the observed strong melting of ground ice continues, the situation has to be reconsidered due to the strong geomorphological dynamics and the sediment structure of the moraine. The hazard potential would be particularly increased by the formation of a lake in front or at the surface of the glacier tongue.

5. Conclusions

Debris-covered glaciers usually build up large moraine dams over tens to thousands of years. In a number of cases, such moraine dams were at the origin of debris flows. Repeated advances and retreats of a glacier reworks till and ice deposits. The latter can resist melting under a suffciently thick till cover for long periods. In the case of a readvancing glacier over dead ice the position of the terminus becomes unclear.

The present study integrates several methods to investigate ongoing geomorphic processes in the forefield of Rossboden Glacier, taking advantage of each specific method. Geophysical means allow to investigate the internal structure of such a glacier forefield and to assess the stability of a moraine where subsurface ice, a possible water table and zones with loosely

bedded material are of particular interest. In addition, the processing of annually taken air photographs by photogrammetry proves to be an ideal complementary method, because it allows to reconstruct processes which have led to the situation encountered at the time of the geophysical field work.

The goal of this study was to investigate internal structures of the moraine, first to determine the active terminus position and second to locate potential mass moving zones. According to the refraction seismic velocities, several formations of glacier deposits could be distinguished: dry and loose moraine, wet and/or consolidated moraine, ice (possibly of multiple origin) and ice/debris mixture. In the steep frontal part of the Rossboden moraine, no indication for a water-saturated formation near the surface was detected. DC resistivity soundings generally showed a continuous increase of resistivities toward the glacier. However, an interpretation of layers in terms of structure and composition remains ambiguous, because data were interpreted assuming a one-dimensional structure, which is critical when large local, especially lateral, anomalies occur. The combination of seismic and geoelectrical methods led to a mutually improved interpretation in terms of assigning material characteristics to the detected layers. An empirical index I calculated from resistivity and seismic velocity reveals whether the investigated subsurface is water-saturated or contains large air voids, both of which are critical parameters in the assessment of the stability of large sediment bodies such as steep moraines. The analysis of the ambient seismic noise, carried out as a test of the method in high-alpine terrain, yielded results that support the findings of the refraction seismics and the DC resistivity soundings regarding the degree of consolidation of the sediments and the occurrence of ice. Further application of this method to less complex underground will help to improve its suitability for this kind of investigation. Photogrammetry confirmed that Rossboden Glacier advanced until at least 1992, when most observed Swiss glaciers have already been retreating for several years. Since then, the debris covered surface subsided markedly due to continuous ice melting. A dead ice mass in front of and separated from the active glacier could be identified by photogrammetrical means.

According to the results of this study, the terminus of the active glacier in 1997 was situated about 400 m behind the ridge of the moraine dam. The moraine dam at Rossboden Glacier is most likely stable in the near future. However, the observed strong melting would require a re-evaluation within a few years.

Acknowledgements

Special thanks go to Françoise Funk-Salamí for the field acquisition, processing and interpretation of the DC resistivity data, to Hermann Bösch for many hours spent in the field and on the interpretation of aerial photographs and plotting of the results, and to Donat Fäh for instructions about and help with the ambient seismic noise analysis. We very much thank Reynald Delaloye, Roland Eichenberger, Anja Fleig, Paul Flück, Frederik Fuchs, Michael Fuchs, Sämi Gähwiler, Adrian Gilli, Andreas Huwiler, Claudine Naguel, Tom Rüegger and Maura Vonmoos for their great commitment as field assistants and Bruno Nedela for drawing figure 6. We are grateful for the generous help provided by the municipal administration of Simplon Dorf. We very much appreciate the logistic support with power supply and storing of explosives by Zenklusen AG, building contractors in Simplon Dorf. Jörg Schäfer's comments improved the early manuscript. We thank François Marillier, Michel Vallon and Wilfried Haeberli for their helpful reviews. This work was financially supported by the Glaciology section of VAW/ETH Zürich. Contribution No. 1267 of the Institute of Geophysics, ETH Hönggerberg, CH-8093 Zürich, Switzerland.

REFERENCES

BARD, P.-Y., & BOUCHON, M., 1985: The two-dimensional resonance of sediment-filled valleys. Bull. Seismol. Soc. America 75 (2), 519–541.

BEARTH, P., 1973: Geologischer Atlas der Schweiz, 1:25'000, Blatt Simplon, mit Erläuterungen. Schweiz. Geol. Kommission.

BLANKENSHIP, D.D., BENTLEY, C.R., ROONEY, S.T., & ALLEY, R.B., 1987: Till beneath ice stream B, 1. Properties derived from seismic travel times. J. Geophys. Res. 92 (B9), 8903–8911.

DOBRIN, M.B., & SAVIT, C.H., 1988: Introduction to geophysical prospecting. McGraw-Hill, New York, 867p.

FÄH, D., RÜTTENER, E., NOACK, T., & KRUSPAN, P., 1997: Microzonation of the city of Basel. J. Seismol. 1, 87–101.

HAEBERLI, W., 1973: Die Basis-Temperatur der winterlichen Schneedecke als möglicher Indikator für die Verbreitung von Permafrost. Z. Gletscherkd. Glazialgeol. 9 (1–2), 221–227.

– 1992: Zur Stabilität von Moränenseen in hochalpinen Getschergebieten. Wasser, Energie, Luft 84. Jg., 11/12, 361–364.

– 1999: Hangstabilitätsprobleme im Zusammenhang mit Gletscherschwund und Permafrostdegradation im Hochgebirge. Relief Boden Paläoklima 14, 11–30.

HAEBERLI, W., & PATZELT, G., 1982: Permafrostkartierung im Gebiet der Hochebenenkarblockgletscher, Obergurgl, Ötztaler Alpen. Z. Gletscherkd. Glazialgeol. 18 (1), 127–150.

HAEBERLI, W., & FISCH, W., 1984: Electrical resistivity soundings of glacier beds: A test study on Grubengletscher, Wallis, Swiss Alps. J. Glaciol. 30 (106), 373–376.

HAEBERLI, W., RICKENMANN, D., ZIMMERMANN, M., & RÖSLI, U., 1990: Investigation of 1987 debris flows in the Swiss Alps: general concept and geophysical soundings. In: R.O. SINNIGER, M. MONBARON (eds.), Hydrology in mountainous regions, Vol. 2. IAHS publication No. 194, 303–310.

HAGEDOORN, J.G., 1959: The plus-minus method of interpreting seismic refraction sections. Geophys. Prospecting 7, 158–182.

HANTKE, R., 1983: Eiszeitalter, Band 3: Westliche Ostalpen mit ihrem bayerischen Vorland bis zum Inn-Durchbruch und Südalpen zwischen Dolomiten und Mont Blanc. Ott-Verlag, Thun, 730 p.

HAUCK, C. (2001): Geophysical methods for detecting permafrost in high-mountains. ETH-Diss. Nr. 14163. 191p.

HOELZLE, M., VONDER MÜHLL, D., BAUDER, A. & GUDMUNDSSON, G.H., 1998: Die Gletscher der Schweizer Alpen im Jahr 1996/97. Die Alpen, Monatsbulletin des Schweizerischen Alpenclubs 10, 10–22.

HOELZLE M., WEGMANN, M., & KRUMMENACHER, B., 1999: Miniature temperature dataloggers for mapping and monitoring of permafrost in high mountain areas: First experience from the Swiss Alps. Permafrost & Periglacial Processes 10 (2), 113–124.

HUGGEL, C. 1998: Periglaziale Seen im Luft- und Satellitenbild. Unpublished diploma thesis at the Geography Department of the University Zurich, 102 p.

INTERPEX LTD., 1997: Resix Plus, Ridge regression inversion of DC resistivity data for PCs and compatible machines, Golden, CO, USA.

KÄÄB, A., 1996: Photogrammetrische Analyse zur Früherkennung gletscher- und permafrostbedingter Naturgefahren im Hochgebirge. Mitt. VAW/ETH Zürich 145, 182 p.

KÄÄB, A., & HAEBERLI, W., 1996: Früherkennung und Analyse glazialer Naturgefahren im Gebiet Gruben, Wallis, Schweizer Alpen. Tagungspublikation Interpraevent 1996, 4, 113–122.

KING, L., 1984: Permafrost in Skandinavien. Untersuchungsergebnisse aus Lappland, Jotunheimen und Dovre/Rondane. Heidelberger Geograph. Arb. 76, 174 p.

KOEFOED, O. 1979: Geosounding principles, 1: Resistivity sounding measurements. Elsevier, Amsterdam, 276 p.

LICHTENHAHN, C., 1979: Die Verbauung des Fellbaches in der Gemeinde Saas Balen (Wallis). Mitt. VAW 41, 169–176.

LUGON, R., GARDAZ, J.-M., & VONDER MÜHLL, D., 2000: The partial collapse of the Dolent Glacier moraine (Mont Blanc Range, Swiss Alps). Z. Geomorph., N.F., Suppl.-Bd. 122, 191–208.

MILSOM, J., 1996: Field geophysics. 2nd edition, Wiley & Sons, Chichester, 187 p.

MÜLLER, H.-N., 1983: Messungen zum aktuellen Gletschervorstoss und zur Verbreitung von Untergrundeis im Vorfeld des Rossbodengletschers (Simplon, Schweizer Alpen). Innsbrucker Geograph. Stud. 8, 45–58.

NAKAMURA, Y. 1989: A method for dynamic characteristics estimation of the subsurface using microtremor on the ground surface. Q. Rept. Railway Tech. Res. Inst. 30/1, 25–33.

MUSIL, M., MAURER, H., GREEN, A.G., HORSTMEYER, H., NITSCHE, F.O., VONDER MÜHLL, D. & SPRINGMAN S., 2002: Shallow seismic survey of an Alpine rock glacier. Geophysics 67, 1701–1710.

OBERHOLZER, P.S., & SALAMÍ, F.S., 1998: Geophysikalische Untersuchungen der Eisverhältnisse am Rossbodengletscher (Simplongebiet, Wallis). Diploma thesis at the Laboratory for Hydraulics, Hydrology and Glaciology, VAW/ETH Zürich, 180 p.

RÖTHLISBERGER, H., 1979: Glaziologische Arbeiten im Zusammenhang mit den Seeausbrüchen am Grubengletscher, Gemeinde Saas Balen (Wallis). Mitt. VAW 41, 233–256.

VONDER MÜHLL, D., 1993: Geophysikalische Untersuchungen im Permafrost des Oberengadins. Mitt. VAW/ETH Zürich, 122, 222 p.

VONDER MÜHLL, D., HAEBERLI, W., & KLINGELE, E., 1996: Geophysikalische Untersuchungen zur Struktur und Stabilitat eines Moränendammes am Grubengletscher (Wallis). Tagungspublikation Interpraevent 1996, 4, 123–132.

VONDER MÜHLL, D., STUCKI, TH. & HAEBERLI, W., 1998: Borehole temperatures in Alpine permafrost: A ten year series. Proceedings Seventh International Conference on Permafrost, 1998, Yellowknife, Canada, 1089–1095.

ZIMMERMANN, M., 1990: Debris flows 1987 in Switzerland: geomorphological and meteorological aspects. In: R.O. SINNIGER, M. MONBARON (Ed.), Hydrology in mountainous regions, Vol. 2. IAHS publication No. 194, 387–393.

Manuscript received October 10, 2001
Revision accepted February 14, 2003